

Optical Engineering

SPIDigitalLibrary.org/oe

Construction and performance of an optical phase and frequency lock of diode lasers

Tomasz Kawalec
Dobrosława Bartoszek-Bober



Construction and performance of an optical phase and frequency lock of diode lasers

Tomasz Kawalec

Dobrosława Bartoszek-Bober

Jagiellonian University

Marian Smoluchowski Institute of Physics

Reymonta 4, 30-059 Krakow, Poland

E-mail: tomasz.kawalec@uj.edu.pl

Abstract. The relative phase and frequency stabilization setups for diode lasers are discussed. The construction and performance of an optical phase lock loop based on integrated phase-locked loop chips are shown along with practical tips facilitating its preparation. The interference pattern between two electronically locked lasers is shown as a proof of the system stability. The fringes contrast is a quantitative indicator of the mean-square phase error. Finally, an example of a very simple frequency offset lock realized with an all-in-one radio chip is also provided. © 2013 Society of Photo-Optical Instrumentation Engineers (SPIE) [DOI: [10.1117/1.OE.52.12.126105](https://doi.org/10.1117/1.OE.52.12.126105)]

Subject terms: optical phase lock loop; diode lasers; optical interference.

Paper 131449 received Sep. 18, 2013; revised manuscript received Nov. 12, 2013; accepted for publication Nov. 18, 2013; published online Dec. 16, 2013.

1 Introduction

The history of the development of the laser phase and frequency stabilization techniques started about 50 years ago.^{1,2} One of the widely used techniques is to stabilize the phase of the beat note signal of two lasers to a highly stable reference generator using a phase-locked loop (PLL). In this case, the error signal of a sufficient bandwidth, produced by a phase-frequency detector, controls the phase and frequency of one of the lasers. Several electronic circuits have been proposed and tested allowing one to stabilize the laser relative frequency in the range of up to several gigahertz.³⁻⁷ A useful model of a digital and analog phase-frequency detector for diode lasers was developed as well.⁸

On the other hand, a frequency offset locking technique provides a rough beat note frequency stabilization with a stability usually better than 1 MHz. A system employing a side of filter frequency detector⁹ and a frequency-to-voltage converter^{10,11} was constructed. An interesting, but quite complicated system consisting of several integrated circuits was developed, where a digital counter of the beat note signal is employed.¹² Simple devices using a delay line made of a coaxial cable and a frequency mixer were also created.^{13,14}

The setups mentioned above provide a relative laser frequency stabilization only. Reviews of some of the techniques for absolute frequency control may be found elsewhere.^{15,16} If the frequency of the laser is stabilized on an absolute scale by other means (e.g., using an optical cavity^{17,18}) then the PLL circuits may serve to transfer this stability to other lasers.

In this paper, we analyze the performance of a locking circuit built on the basis of cheap universal phase-frequency detectors devoted originally to wireless communication. The importance of the reference generator noise and the frequency agility of the system are discussed. Several practical advices are also given to facilitate and optimize the construction of the locking system. An interferometric method is shown which allows a direct observation of the locking system stability using half of a Mach-Zehnder interferometer

and one acousto-optic modulator (AOM). The contrast of the interference fringes is a quantitative indicator of the mean-square phase error, being a measure of the system quality.

For simple applications where only the mean frequency stability is required, a very simple frequency offset lock based on an all-in-one chip with the minimal number of external electronic components is presented.

2 Experimental Setup

The general idea of a simple but efficient optical PLL for diode lasers is based on a circuit presented by Appel et al.⁶ The main parts of the locking system are shown in Fig. 1(a). The beams from L1 (master) and L2 (slave) lasers (Littrow configuration Toptica DL100 and oscillator-amplifier Toptica TA pro, respectively) are sent on a fast photodiode. During the tests, we have used either the oscillator or amplifier output of the L2 laser. For beat note frequencies of up to 3 GHz, the Alphalas UPD-200-UP photodiode was used and UPD-30-VSG-P model in the 3 to 7 GHz range. To maximize the beat note signal, the beams have to be of the same linear polarization and direction with an angular accuracy better than $\alpha_0 = \lambda/d$ in a plane wave approximation, where λ is the wavelength of the laser light and d is the diameter of the photodiode—see Fig. 1(b).¹⁹ In our case α_0 was about 2.6 mrad and the angle α between the beams was no greater than 1 mrad. The power of both beams was in the range of 0.5 to 8 mW.

The photodiode is followed by a wideband fast amplifier consisting of four units based on ERA-1 chips (Mini-Circuits ZJL-7G or homemade ones). The amplified beat note signal is fed into a spectrum analyzer SA (Rigol DSA1030A) and a PLL circuit with either ADF4002 or ADF4007 Analog Devices chips. The beat note signal frequency is internally divided by N in a digital divider and phase stabilized to the external reference signal, provided by a digital 25 MHz Tektronix AFG3022B, 1 GHz Hewlett-Packard HP8647A, or single frequency crystal generator. The reference signal frequency is internally divided by R before passing it to the phase-frequency detector. The ADF4002 chip was used with an evaluation board EV-ADF4002SD1Z. The N and R

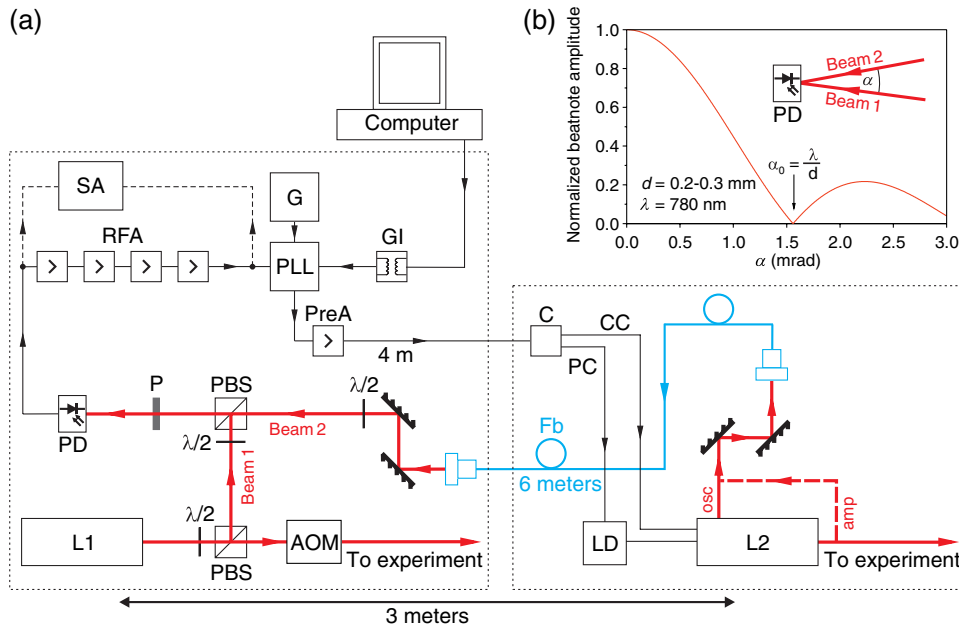


Fig. 1 (a) Simplified sketch of the setup. Some beam guiding mirrors, optical isolators, lenses and half waveplates are omitted: AOM—double-pass acousto-optic modulator (see Sec. 4), C—controller card with current (CC) and piezo (PC) control outputs, Fb—single mode optical fiber with couplers, G—digital function generator (Tektronix AFG3022B or HP8647A), GI—galvanic isolation (Analog Devices ADuM1300), LD—laser piezo driver, L1—Toptica DL 100 laser, L2—Toptica TA pro laser with oscillator (osc) and amplifier (amp) outputs, $\lambda/2$ —half waveplate, P—polarizer, PBS—polarization beam splitter, PD—fast photodiode (Alphas UPD-200-UP or UPD-30-VSG-P), PLL—phase-locked loop circuit, PreA—preamplifier, RFA—fast amplifiers, SA—spectrum analyzer (Rigol DSA1030A). The dotted rectangles denote two separate optical tables. (b) Calculated normalized beat note amplitude on a PD photodiode as a function of the angle α between beams 1 and 2.

divider, as well as other parameters, were computer controlled by a dedicated software via three-channel digital link. To avoid ground loops when using two different electric networks, it was absolutely necessary to use a galvanic isolation (Analog Devices ADuM1300 digital triple-channel magnetically coupled isolator). The ADF4007 chip was used either with a dedicated evaluation board (EVAL-ADF4007EBZ1) or on a small (4×4 cm, 0.6-mm thick) printed circuit board (PCB) provided mainly for amateur use in the gigahertz range. There are only four settings of N divider (8, 16, 32, and 64 chosen with jumper switches) and R is permanently set to 2.

The PLL charge pump signal is amplified in a preamplifier (PreA) and sent to a card C—see Fig. 2. The PreA matches the charge pump output with a low impedance of the C card input, has a flat characteristics up to 7 MHz, and gives 2.6 dB amplification at a frequency of 500 kHz. A simple series resistor-capacitor (RC) low pass filter was usually used at the output of the charge pump with experimentally found values of 900 Ω and 4.7 nF. The main purpose of the C card is to split the error signal into two branches. The first one, called “slow,” consists of an integrator with a stepwise variable time constant and a regulated amplifier and controls roughly the L2 laser frequency via piezo actuator with a bandwidth of up to

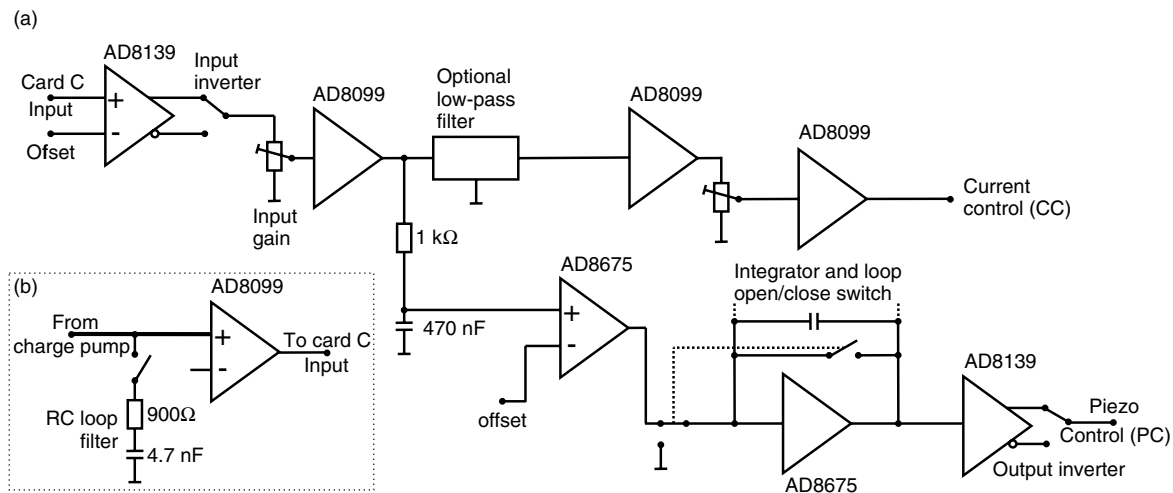


Fig. 2 A simplified block scheme of the card C (a) and the PreA (b). The offset voltages are generated with digital-to-analog converters controlled by the Atmega8 chip. All the switches are realized with IM06 AXICOM relays. The capacitors in the integrator are chosen with manual microswitches.

10 kHz. The second branch (the “fast” or “current” one) amplifies the error signal in a wideband regulated amplifier and directly feeds the DC-coupled current modulation input of L2 laser head (factory mounted “mod DC”). The current branch is optionally low pass filtered with an inductor-capacitor (LC) filter to reduce reference spurs. The LC filter corner frequency is 3 to 30 MHz and its attenuation is 12 dB/octave. The filter may be switched on and off with a pair of relays.

The input signal of the C card and the output signal of the piezo branch may be inverted due to the relays switching between complementary outputs of the operational amplifiers. The purpose of this option is twofold. First, the input signal inversion allows the slave laser to be locked on demand either below or above the frequency of the master laser. Second, the combination of the two inverters allows one to use various types of the current and piezo slave laser drivers (i.e., with any direction of the laser frequency change with the input steering voltage). The C card is thus very flexible regarding both the locking range and the slave laser driver configurations.

All the relays, as well as the input signal offset, are conveniently controlled by a microcontroller with a very simple user interface consisting of three mini push button switches. The amplification of the input circuit, the current, and the piezo branch are regulated with multiturn potentiometers. The time constant of the slow branch integrator is controlled by a set of dip switches.

The measured K_O parameter of the L2 laser (corresponding to an oscillator gain in a classical PLL loop) was 0.74 MHz/mV for the DC input voltage.

The L1 and L2 lasers were mounted on two separate optical tables and powered from two different electric networks. Due to the geometry of the setup, a few propagation delays in the PLL loop were introduced in addition to the intrinsic phase-frequency detector delay. In particular, optical fibers contribution is 30 ns, air path—10 ns, BNC cables—45 ns, C card and electronics—15 ns, giving in total about 100 ns of loop delay.

A typical spectra of the beat note signal are presented in Fig. 3 in a logarithmic vertical scale. The relative spectrum of unlocked L1 and L2 lasers is shown in Fig. 3(a) whereas the spectrum of piezo locked lasers is shown in Fig. 3(b). If only the piezo branch is employed, the loop oscillates in the kilohertz range causing the spectrum broadening. However, the current branch finally recovers the loop stability, as seen in Fig. 3(c). The width of the main central peak was confirmed to be <math><1\text{ Hz}</math> with a Tektronix RSA3308 spectrum analyzer. The broad pedestal is formed by a residual noise. The width of this pedestal gives a rough estimation of the bandwidth of the loop whereas the side maxima correspond to the natural frequency of the loop. Small peaks at $100 \pm 25\text{ MHz}</math> indicate the presence of reference spurs.$

3 Performance of the System

The effective locking range of the system based on ADF4002 was found to be 30 to 500 MHz. The capture range depends on the chosen f_{bn} beat note frequency to be stabilized and was, for example, -400 to $600\text{ MHz}</math> for $f_{bn} = 400\text{ MHz}</math> and -200 to $600\text{ MHz}</math> for $f_{bn} = 200\text{ MHz}</math>. The ADF4007 system locking range was proven to be about $200\text{ MHz}</math> to $7\text{ GHz}</math>, with a capture range of at least $\pm 2.5\text{ GHz}</math>.$$$$$$$

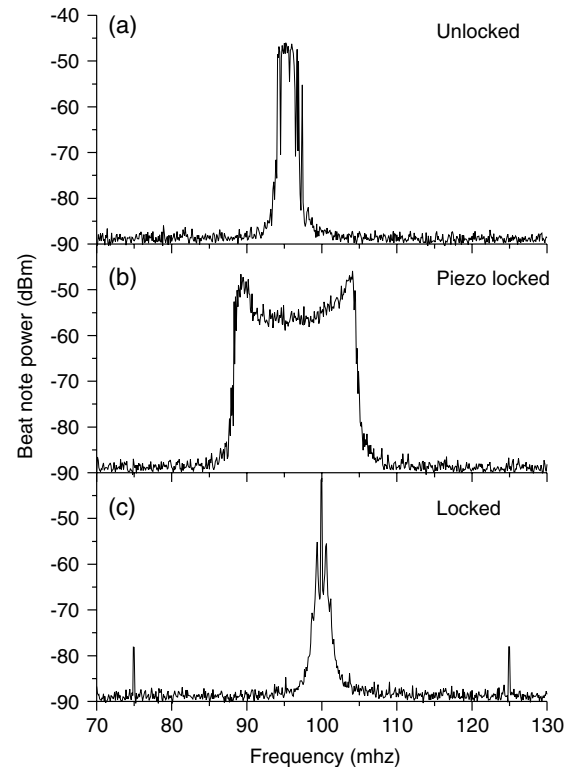


Fig. 3 Typical power spectra of a beat note signal on a PD photodiode: (a) the PLL is completely opened, (b) the laser is only piezo stabilized, and (c) piezo and current loops are closed. $N = 4$, reference frequency $f_{ref} = 25\text{ MHz}</math>.$

A common measure of the quality of the relative phase stabilization is $\langle \Delta\phi^2 \rangle$, being a mean-square phase error. Alternatively, one can consider the ratio Q of the power in the central peak of the beat note spectrum to the total power in the whole beat note signal (i.e., central peak plus noise background). Assuming $\langle \Delta\phi^2 \rangle \ll 1$, a simple relation $Q = e^{-\langle \Delta\phi^2 \rangle}$ is valid.⁸

In practice, we have calculated Q using the total power of the spectrum found in the following way. For each Q measurement, we have recorded three spectra centered at the main beat note peak with the span (1) 6 MHz, (2) 50 kHz, and (3) 10 kHz and a resolution bandwidth 3 kHz, 300 Hz, and 100 Hz, respectively. Root mean square (RMS) detector was used in each measurement and video bandwidth was set to $10 \times \text{RBW}</math> to avoid noise level underestimation. Each spectrum was normalized by subtracting $10 \log(\text{RBW})</math>. The central part of the spectrum (1) was then replaced with the spectra (2) and (3). This way the whole spectrum was effectively measured with a greater resolution at the center and a lower resolution where only a slowly varying noise spectrum was present. Finally, the spectra were integrated with respect to the frequency giving the total power of the beat note signal. Typical values of Q and $\langle \Delta\phi^2 \rangle$ in our system are 90% and 0.10, respectively, and are comparable with the values reported for other circuits.^{7,8}$$

Typical beat note spectra for various system parameters are shown in Fig. 4. The crucial parameter governing the system performance is the loop amplification. The “amplification” parameter in the figure denotes the total voltage amplification of the PreA and C card current branch. If it is too low then the current loop does not suppress the piezo loop oscillations—

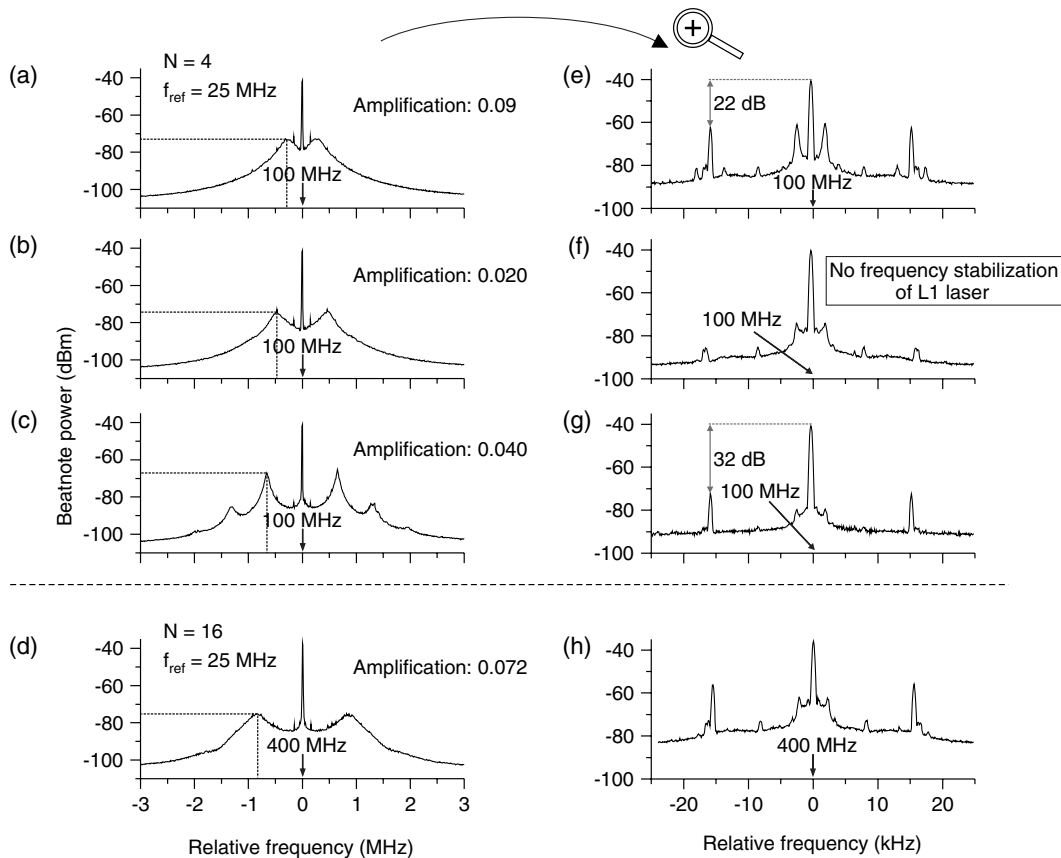


Fig. 4 Close look at the beat note signal power spectra for different current loop amplifications: (a)–(d) 6 MHz span and (e)–(h) 50 kHz span. In the last row no loop filter was used whereas the remaining data were collected with a simple series RC filter placed in front of the PreA. The total amplification of the error signal between the charge pump output and the laser current input is also listed.

see Fig. 3(b). In the opposite case, as it is well known, the stability criterion is not met in the current loop, leading to huge oscillations and dramatic widening of the beat note spectrum.

For a stable loop, the side peaks of the spectrum move away from the main peak and their amplitude increases with an increasing amplification in the loop—see the dotted lines in Figs. 4(a)–4(c) provided to guide the eye. It was found that the best system performance is achieved when using the highest amplification which does not generate harmonics of the natural loop frequency, seen in Fig. 4(c). In particular, the improper (too high or too low) loop amplification lowers the Q ratio by up to 25 percentage points. The widest loop bandwidth [see Fig. 4(d)] is in the absence of the dedicated RC loop filter at a price of a much lower system stability and a very narrow range (a few percentages) of usable loop amplifications. The RC loop filter is requisite for beat note frequencies lower than about 100 MHz. Several representative values of Q , $\langle \Delta\phi^2 \rangle$ and loop amplifications are presented in Table 1 for various system configurations.

The peaks at ± 15.5 kHz in Figs. 4(e), 4(g), and 4(h) come from a slight FM modulation of the L1 laser frequency, used for its frequency stabilization in a standard Doppler-free absorption spectroscopy setup.¹⁶ The spectrum collected without L1 laser stabilization is shown for comparison—see Fig. 4(f).

The part of the spectrum in the close vicinity of a main peak in Figs. 4(e)–4(h) depends on the current loop amplification as well as the piezo loop amplification and its

bandwidth. However, the parameters of the piezo path are not critical for the overall system performance. The amplification should be high enough to roughly keep the laser at a desired frequency in the presence of the inherent L2 laser long-term instability and L1 laser optional frequency scan. The optimal piezo loop parameters may be found experimentally aiming at a reduction of the residual pedestal seen in the central part of Figs. 4(e)–4(h).

The quality of the laser locking depends strongly on the noise parameters of the reference generator and the N factor (where N is the division factor of the beat note signal frequency). We have compared the beat note spectra of the same central frequency f_{bn} but generated with different N , reference generators, and reference frequencies f_{ref} . An exemplary result is shown in Fig. 5 for $f_{bn} = 800$ MHz. For small N , the $\langle \Delta\phi^2 \rangle$ is low (0.14) for the HP reference generator and $f_{ref} = 200$ MHz—see curve (1). In contrast, for a high N equal 64 ($f_{ref} = 25$ MHz here) the $\langle \Delta\phi^2 \rangle$ parameter depends strongly on the generator inherent noise (see inset of Fig. 5) and equals 0.19 ($Q = 83\%$) for AFG generator (curve 2) and 0.65 ($Q = 52\%$ only) for HP generator (curve 3). $\langle \Delta\phi^2 \rangle$ is affected mainly by the noise present in the nearest neighborhood of the main peak in the beat note spectrum. Indeed, the curves (2) and (3) are identical except for the central ± 10 kHz part. The small peaks on both sides of the central peak presumably appear as a result of a coupling between digital and analog parts of the phase-frequency detector.

The reference spurs are seen for relatively low reference frequencies, mainly in ADF4007 based system. Their

Table 1 Exemplary data of the PLL performance; f_{ref} denotes the reference frequency and f_{bn} the beat note frequency.

ADF chip	Reference generator	N	f_{ref} (f_{bn}) (MHz)	Loop amplification	$\langle \Delta\phi^2 \rangle$ (Q) (rad ²) (%)
With RC loop filter, no low pass LC filter					
4007	AFG3022B	64	25 (800)	0.490	0.19 (83)
4007	HP8647A	64	25 (800)	0.490	0.65 (52)
4007	HP8647A	8	200 (800)	0.150	0.14 (87)
4007	HP8647A	32	170 (2720)	0.450	0.20 (82)
4002	AFG3022B	2 ÷ 16	25 (50 ÷ 400)	0.026 ÷ 0.175	≈0.10 ± 0.02 (90 ± 3)
4002	Crystal oscillator	8	32 (256)	0.10	0.11 (90)
With RC loop filter and low pass LC filter					
4002	AFG3022B	16	25 (400)	0.160	0.14 (87)
No filters					
4002	AFG3022B	16	25 (400)	0.090	0.13 (88)

amplitude is 20 to 40 dB lower than the amplitude of the beat note for reference frequencies ranging from 15 up to a few tens of megahertz. When an optional low pass LC filter was inserted in the current path in the C card, the reference spurs were reduced by 2 to 25 dB at a cost of a very slight increase of $\langle \Delta\phi^2 \rangle$ (see Table 1 for representative data). The optimal corner frequency of the filter was found to be 10 MHz.

3.1 Frequency Agility

A frequency agility of the system was measured by recording the closed-loop error signal response to a sudden change in

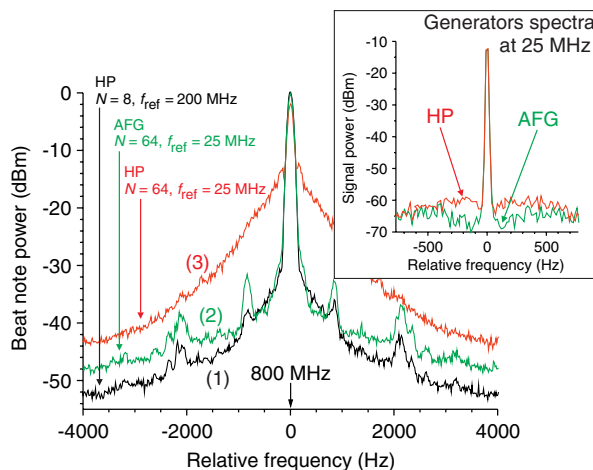


Fig. 5 The power spectra of the beat note signal for two different reference generators and two values of N in ADF4007 system. The inset shows the spectra of the HP8647A and AFG3022B generators set to 25 MHz (RBW—100 Hz, acquisition time—600 s). See Sec. 3 for discussion.

the reference frequency. Additionally, the instantaneous beat note frequency was measured at different moments with a 5 Gs/s oscilloscope to precisely find the appearance of the relocking state. A number of N multipliers and reference frequency steps were tested with the highest change in the beat note frequency f_{bn} equal $16 \times 12 \text{ MHz} = 192 \text{ MHz}$. After the reference frequency jump, both the current and piezo loop try to shift the L2 slave laser frequency to a new value. However, for low current loop amplification, the maximal change in the frequency forced by the current branch is low as well (i.e., the maximal error signal voltage times amplification is too low). In this case, the beat note frequency rate of change is governed mainly by the piezo branch and was found to be about 110 MHz/ms. On the other hand, for small beat note frequency steps of up to 50 MHz in our case, when the laser frequency may be controlled primarily by the current loop, the rate of frequency change was found to be 1 to 1.5 GHz/ms.

3.2 Practical Hints

If an efficient and flexible phase-frequency locking of the beat note signal are required, a low noise stable reference generator is absolutely necessary, as described in the previous sections. A sine waveform was found to be a slightly better choice in comparison to a square one. However, in applications where a fixed beat note frequency is sufficient, a total cost of the system may be significantly lowered when using a cheap crystal oscillator as a source of the reference signal. We have tested a FUJI ELECTRIC FXO-111-32 MHz crystal oscillator disassembled from an old computer card. The oscillator signal was filtered out with a Chebyshev II-type LC filter to reduce harmonic components. The system performance was the same as for digital function generator. Although some of the ADF chips' family, including ADF4002, allow the use of rational numbers N/R as

reference frequency multipliers (R is the division factor of the reference signal frequency), one has to be aware that for low f_{ref}/R values a set of strong reference spurs is present in the beat note spectrum. If the condition of the beat note frequency stability may be relaxed, like for a repumping laser in cold atoms field, then a voltage controlled oscillator (VCO) reference generator, like Mini-Circuits POS-150, was proven to be a good choice.

It was found that the loop based on an ADF4007 chip mounted on a small amateur PCB tends to oscillate at a lower loop gain than it does in the case of a dedicated evaluation board due to a suboptimal circuit design. Nevertheless, this system was able to lock the ^{87}Rb cooling and repumping lasers with a frequency difference of almost 7 GHz.

We have found no difference in the performance of the system when using either oscillator (seed laser) or amplifier output of the TA pro L2 laser (see lower right corner of Fig. 1), reaching in both cases $\langle \Delta\phi^2 \rangle = 0.10$. The PLL system was also tested with Toptica DLX110 as the L2 laser, showing slightly worse performance, presumably due to a poor L2 laser operation—its spectral width was a few megahertz.

An additional RC parallel phase advance filter placed in the current loop increases the loop bandwidth but does not improve in our system the $\langle \Delta\phi^2 \rangle$ parameter, presumably due to a large loop delay.

The flexibility of the PLL system was proven in a simple test. The setup was simplified by removing the C card. The PreA was connected to the current input of the L2 slave laser head through a multiturn potentiometer providing a regulated amplification of <1 . The measured performance of the system was the same as previously ($\langle \Delta\phi^2 \rangle = 0.09$, $Q = 91\%$), excepting a small capture range (a few tens of megahertz only) and a low long-term stability due to the lack of a piezo control. Thus, for the general purpose PLL system for diode lasers, the exact realization of the error signal path is not critical. The main factor governing the system performance is the loop amplification and the reference generator noise. The important factor limiting the usable loop amplification is the loop delay, determined mainly by the experiment geometry and the quality of the PCB hosting the PLL chips. The loop remains stable for many hours of operation and the system with both ADF chips has been used successfully in experiments with cold atoms on a daily basis. In particular, it controls in the wide range the frequency of the laser creating the dipole mirror for cold atoms²⁰ and the main cooling laser in the compact system for the production of a Bose-Einstein condensate on an atom chip (Cold Quanta RuBECiTM).

4 Direct Observation of the Locking Performance

The performance of the PLL system may be directly shown by taking advantage of the interference phenomenon.²¹ The L1 and L2 beams denoted “to experiment” in Fig. 1(a) were spatially filtered with the optical single mode fibers, aligned perpendicularly to each other and sent on a glass plate, forming just a half of a Mach-Zehnder interferometer—with a beam combiner only. In order to observe stable fringes visible to a naked eye it is necessary to equal the frequency of both beams. This was done by adding an AOM in the double-pass configuration in the path of the L1 laser beam. The PLL frequency difference was set to 200 MHz ($N = 10$, $f_{\text{ref}} =$

20 MHz) and the AOM frequency to 100 MHz. The generator driving the AOM and the PLL reference generator were synchronized via a standard 10 MHz link to improve the fringes’ stability. The interference fringes for two locking conditions are shown in Fig. 6. In Fig. 6(a), the optimal locking condition was used, whereas in Fig. 6(b) the loop amplification was reduced. The cross sections of the fringes averaged over 20 central horizontal lines are presented in Fig. 6(c).

An estimation of the $\langle \Delta\phi^2 \rangle$ may be extracted from the visibility V of the interference fringes.²² Taking into account two parallel interfering beams, shifted in phase by $\phi + \Delta\phi$, the interference pattern and the visibility V are easy to calculate ($\Delta\phi$ is a temporary phase deviation). Assuming the following constraints: (1) equal intensity of both interfering beams, (2) $\langle \Delta\phi \rangle = 0$, (3) $|\Delta\phi| \ll 1$, and (4) $\langle \Delta\phi^2 \rangle \ll 1$, one gets: $\langle \Delta\phi^2 \rangle = 2(1 - V)$. This equation is approximately valid also if the conditions (3) and (4) are partially relaxed.

The $\langle \Delta\phi^2 \rangle$ calculated from the fringes’ contrast and the spectrum analyzer measurements are in very good agreement. For example, for data shown in Fig. 6, $\langle \Delta\phi^2 \rangle$ equals 0.14 ± 0.03 and 0.94 ± 0.05 in (a) and (b), respectively. The corresponding values calculated from the beat note spectra are 0.14 ± 0.02 and 1.12 ± 0.05 .

5 Simplified Scheme for Frequency Stabilization

An even simpler yet less flexible electronic circuit was also tested. Its heart was a radio receiver all-in-one PLL synthesizer chip TSA6057. Due to its low bandwidth, it is able to provide only a mean frequency offset locking rather than a phase one in the case of diode lasers. The chip was used in its typical configuration in the so-called FM mode (30–150 MHz nominal range) with a few passive elements and a 5 MHz quartz reference. The error signal was sent via PreA to the card C. Since in this chip, the error signal is updated with the frequency equal the synthesizer tuning step, the maximal available step of 31.25 kHz was chosen. In this case, as for the ADF family chips, the loop

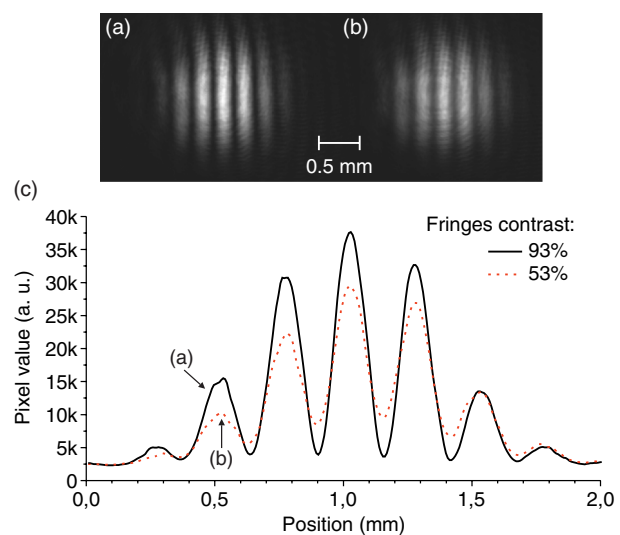


Fig. 6 Image of the two-laser interference fringes taken with a CCD camera for two different frequency locking conditions (a and b), see text for details. The cross section of the fringes is shown in (c). The CCD integration time was 50 ms. The loop parameters were $N = 10$, $f_{\text{ref}} = 20$ MHz.

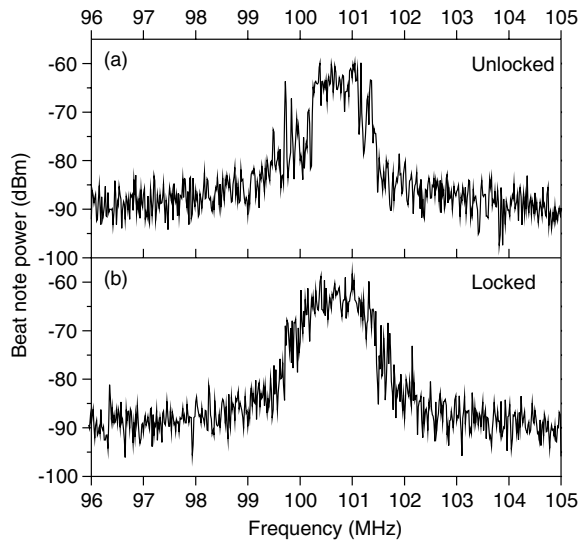


Fig. 7 Typical power spectra of a beat note signal for a common radio all-in-one PLL TSA6057 chip: (a) open loop, (b) piezo and current loop closed; RBW—10 kHz, detector—RMS average.

oscillations appearing in the piezo locked loop were suppressed by the current branch. The beat note spectra for the open and closed loops are shown in Fig. 7. The mean beat note frequency stability depends on the stability of the crystal resonator used and is on the order of 0.1%. The envelope of the beat note signal shown in part (b) is a little bit broader than the instantaneous signal width in part (a), due to a low bandwidth of the system, preventing suppression of the fast frequency fluctuations.

The TSA6057 chip is an obsolete part, however, we have proven here that similar components might be used in simple applications. The main drawback of this solution is a small tuning and capture range of 40 to 160 MHz only. Nevertheless, we have successfully employed it in an optical dipole mirror for cold rubidium atoms described elsewhere.²⁰

6 Summary

We have shown that the PLL systems based on integrated chips are very flexible and easy to implement in diode lasers used in atom optics experiments. The phase-frequency locking efficiency and frequency agility were investigated for a wide range of parameters and configurations. In particular, we have directly shown the influence of the reference generator noise on the system performance. The lowest mean-square phase error $\langle \Delta\phi^2 \rangle$ is $<0.1 \text{ rad}^2$ despite relatively long spatial and optical distances between lasers. Such a low value makes the system useful for atomic coherence experiments.⁵

A set of practical solutions was given, including a simple circuit for frequency offset locking with on-demand red or blue detuning. We have also presented a simple interferometric method allowing one to quantitatively control the system stability. A frequency offset lock based on a radio all-in-one synthesizer was proposed and tested as well.

Acknowledgments

Financial support by the Polish Ministry of Science and Higher Education (Grant No N N202 124536) and National Science Centre (Grant No 2011/01/N/ST2/00479) is

gratefully acknowledged. Part of the equipment was purchased thanks to the financial support of the European Regional Development Fund in the framework of the Polish Innovation Economy Operational Program (POIG.02.02.00-00-003/08 contract). We are grateful to Aleksandra Plawecka for help with the interferometry experiment and to colleagues from the Photonics Department for lending us a high-frequency generator. We thank Analog Devices for the samples of ADF4007 and ADuM1300 chips.

References

1. J. L. Hall, "Stabilized lasers and precision-measurements," *Science* **202**(4364), 147–156 (1978).
2. J. L. Hall, "Laser absolute wavelength standard problem," *IEEE J. Quantum Electron.* **QE-4**(10), 638–641 (1968).
3. J. L. Hall, M. Long-Sheng, and G. Kramer, "Principles of optical phase-locking—application to internal mirror He-Ne lasers phase-locked via fast control of the discharge current," *IEEE J. Quantum Electron.* **23**(3), 427–437 (1987).
4. D. Höckel, M. Scholz, and O. Benson, "A robust phase-locked diode laser system for EIT experiments in cesium," *Appl. Phys. B* **94**(3), 429–435 (2009).
5. A. M. Marino and C. R. Stroud Jr., "Phase-locked laser system for use in atomic coherence experiments," *Rev. Sci. Instrum.* **79**(1), 013104 (2008).
6. J. Appel, A. MacRae, and A. I. Lvovsky, "A versatile digital GHz phase lock for external cavity diode lasers," *Meas. Sci. Technol.* **20**(5), 055302 (2009).
7. L. Cacciapuoti et al., "Analog plus digital phase and frequency detector for phase locking of diode lasers," *Rev. Sci. Instrum.* **76**(5), 053111 (2005).
8. M. Prevedelli, T. Freearge, and T. W. Hänsch, "Phase-locking of grating-tuned diode lasers," *Appl. Phys. B* **60**(2–3), S241–S248 (1995).
9. G. Ritt et al., "Laser frequency offset locking using a side of filter technique," *Appl. Phys. B* **79**(3), 363–365 (2004).
10. N. Strauß et al., "A simple scheme for precise relative frequency stabilization of lasers," *Appl. Phys. B* **88**(1), 21–28 (2007).
11. T. Stace, A. N. Luiten, and R. P. Kovachich, "Laser offset-frequency locking using a frequency-to-voltage converter," *Meas. Sci. Technol.* **9**(9), 1635–1637 (1998).
12. J. Hughes and C. Fertig, "A widely tunable laser frequency offset lock with digital counting," *Rev. Sci. Instrum.* **79**(10), 103104 (2008).
13. H. N. Rutt, "A heterodyne frequency offset locking technique for pulsed or CW lasers," *J. Phys. E* **17**(8), 704–709 (1984).
14. U. Schünemann et al., "Simple scheme for tunable frequency offset locking of two lasers," *Rev. Sci. Instrum.* **70**(1), 242–243 (1999).
15. G. Galbács, "A review of applications and experimental improvements related to diode laser atomic spectroscopy," *Appl. Spectrosc. Rev.* **41**(3), 259–303 (2006).
16. W. Gawlik and J. Zachorowski, "Stabilization of diode-laser frequency to atomic transitions," *Opt. Appl.* **34**(4), 607–618 (2004).
17. Ch. Salomon, D. Hils, and J. L. Hall, "Laser stabilization at the millihertz level," *J. Opt. Soc. Am. B* **5**(8), 1576–1587 (1988).
18. D. Lisak et al., "Ultra-narrow laser for optical frequency reference," *Acta Phys. Pol. A* **121**(3), 614–621 (2012).
19. J. A. R. Griffith and G. Duxbury, "Laser heterodyne spectroscopy," *Philos. Trans. R. Soc., A* **307**(1500), 563–571 (1982).
20. D. Bartoszek et al., "Optical surface devices for atomic and atom physics," *Opt. Appl.* **40**(3), 535–546 (2010).
21. T. Kawalec and D. Bartoszek-Bober, "Two laser interference visible to the naked eye," *Eur. J. Phys.* **33**(1), 85–90 (2012).
22. E. Kapon et al., "Control of mutual phase locking of monolithically integrated semiconductor lasers," *Appl. Phys. Lett.* **43**(5), 421–423 (1983).

Tomasz Kawalec is an assistant professor at the Faculty of Physics, Astronomy and Applied Computer Science of the Jagiellonian University in Cracow, Poland. He received the MS and PhD degrees in physics from the Jagiellonian University in Cracow in 2001 and 2005, respectively. His field of research is atomic physics, with an emphasis on cold and ultracold atoms.

Dobrosława Bartoszek-Bober graduated as a Master of Science in experimental physics from Jagiellonian University in Cracow, Poland, in 2008. She completed her PhD research in 2013 in the Laboratory of Cold Atoms Near Surfaces in the Marian Smoluchowski Institute of Physics. Currently, she is a postdoc in the National Laboratory of Atomic, Molecular and Optical Physics in Toruń, Poland. Her research interests include cold and ultracold atom physics.